UNIVERSITÉ DE GENÈVE

Archive ouverte UNIGE
https://archive-ouverte.unige.ch

Article scientifique | Article | 2016

Accepted version | Open Access

This is an author manuscript post-peer-reviewing (accepted version) of the original publication. The layout of the published version may differ .

Anion Transport with Chalcogen Bonds

Benz, Sebastian; Macchione, Mariano; Verolet, Quentin; Mareda, Jiri; Sakai, Naomi; Matile, Stefan

How to cite

BENZ, Sebastian et al. Anion Transport with Chalcogen Bonds. In: Journal of the American Chemical Society, 2016, vol. 138, n° 29, p. 9093–9096. doi: 10.1021/jacs.6b05779

This publication URL: https://archive-ouverte.unige.ch/unige:85614
Publication DOI: 10.1021/jacs.6b05779

© This document is protected by copyright. Please refer to copyright holder(s) for terms of use.

Anion Transport with Chalcogen Bonds

Sebastian Benz, Mariano Macchione, Quentin Verolet, Jiri Mareda, Naomi Sakai, and Stefan Matile*

Department of Organic Chemistry, University of Geneva, CH-1211 Geneva, Switzerland

ABSTRACT. In this report, we introduce synthetic anion transporters that operate with chalcogen bonds. Electron-deficient dithieno[3,2-b;2',3'-d]thiophenes (DTTs) are identified as ideal to bind anions in the focal point of the σ holes on the co-facial endocyclic sulfur atoms. Anion binding in solution and anion transport across lipid bilayers are found to increase with the depth of the σ holes of the DTT anionophores. These results introduce DTTs and related architectures as privileged motif to engineer chalcogen bonds into functional systems, complementary in scope to classics such as 2,2'-bipyrroles or 2,2'-bipyridines that operate with hydrogen bonds and lone pairs, respectively.

Synthetic transport systems[1-3] have emerged as an attractive tool to elaborate on the functional relevance of interactions that are otherwise less recognized.[3] Leading examples for such unorthodox interactions at work in lipid bilayer membranes include halogen bonds and anion-π interactions.[3] Here, we report the first example for anion transport with chalcogen bonds.

Chalcogen bonds originate from σ holes on electron-deficient sulfur, selenium or tellurium but not oxygen atoms (Figure 1A).[4-6] With the σ^* orbitals of the two C-X bonds accounting for the σ holes, chalcogen bonds extend co-linear to these bonds, i.e., $\Phi_1 \sim 180°$. This resulting angle between a chalcogen bond and the other, co-planar C-X bond is, with $\Phi_2 \sim 70°$, relatively small. It is perhaps this small Φ_2 that has limited the use of chalcogen bonds in functional systems mostly to intramolecular conformational control and solid-state crystal engineering.[4,5] Anion binding with telluradiazoles in solution has been realized recently.[6]

2,2'-Bithiophenes[7] were considered as conceptually innovative motif for the design of chalcogen-bond transporters and beyond (Figures 1B). On the one hand, they are nicely complementary to 2,2'-bipyridines, the classical motif to bind cations rather than anions with the two nitrogen lone pairs (Figure 1C).[8] On the other hand, they complement 2,2'-bipyrroles (Figure 1D). This classical motif to bind anions with conventional hydrogen rather than unorthodox chalcogen bonds is present also in biological anion transporters such as prodigiosin and synthetic mimics in many variations.[2]

Density functional theory (DFT) modeling at the M062X/6-311G** level of theory[9-11] in the gas phase supported 2,2'-bithiophenes as operational anionophores. Dithieno[3,2-b;2',3'-d]thiophenes (DTTs)[5,12-14] appeared particularly attractive because the orientation of the co-facial σ holes is preorganized, and their bite angle is enlarged. The chalcogen-bond angle in chloride complexes was found to increase correspondingly from $\Phi_1 =$ 149° in 2,2'-bithiophenes (Figure 1F) to $\Phi_1 = 177°$ in DTT **1** (Figures 1F, G). The S-Cl distances decreased correspondingly to end up far below the sum of the VdW radii (3.7 Å; Figures 1F, G). Computed anion binding energies in 1:1 complexes increased with the depth of the σ holes, achieved by oxidation of the bridging "sulfide donors" in DTT **1-2** to "sulfoxides" in DTT-*S*-oxides **3-4** and "sulfone" acceptors in DTT-*S*,*S*-dioxides **5-10** (Figure 1E, Table 1).[5,12-16] DFT models confirmed that one or two vicinal acceptors can further increase anion binding (e.g., **5-7**, Table 1, Figure 1H; **7**: $\Phi_1 = 179°$, S-Cl = 2.9 Å). The addition of hetero-

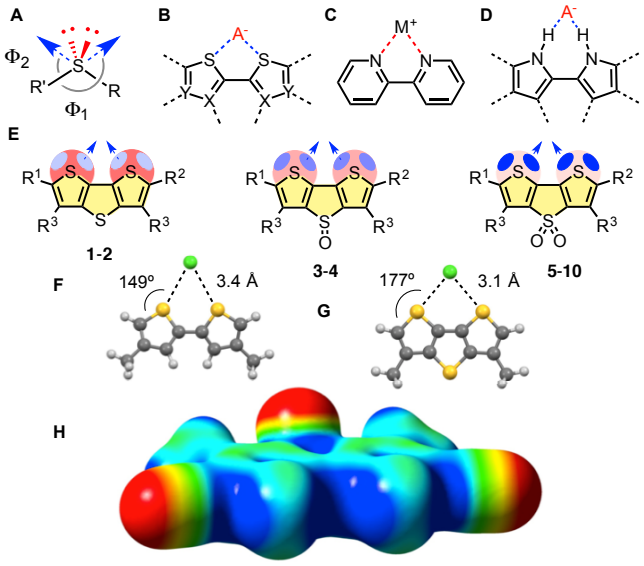

Figure 1. Design of chalcogen-bond anionophores. (A) Directionality of chalcogen bonds (dashed arrows) of sulfur atoms: $\Phi_1 \sim 180°$, $\Phi_2 \sim 70°$. (B-D) Envisioned anion complexes with 2,2'-bithiophenes (B) compared to classical complexes with 2,2'-bipyridines (C) and 2,2'-bipyrroles (D). (E) Structure of the new transporters **1-10** (compare Table 1). (F-G) M062X/6-311G** optimized structures of chloride complexes of 2,2'-bithiophenes (F) and DTT **1** (G). (H) Electrostatic potential surface (EPS) computed at MP2/6-311++G**//M062X/6-311G** level of theory for DTT **7** (R^3 = Me, blue: electron poor, red: electron rich).[11]

atoms in the thiophene ring produced deep σ holes together with strong computed binding. However, all bithiazoles tested were inactive as anion transporters, presumably because they are too hydrophilic to partition into the membranes, and were thus not further investigated (not shown).

DTTs **1-10** were easily accessible by adapting previously reported synthetic procedures (Scheme 1).[13,14] All details on DTT synthesis can be found in the Supporting Information (Schemes S1-S3).[17]

The absorption spectra of DTT **7** in THF showed a maximum at λ_{abs} = 376 nm (Figure 2A). Chloride binding caused appreciable hypo- and bathochromism, whereas the emission at λ_{em} = 444 nm did not shift but was almost completely quenched (Figure 2B). Analysis of dose response isotherms for 1:1 complexes gave a $K_D = 1.13 \pm 0.03$ mM (Figures S1, S2, Table S1). The Job plot supported formation of a 1:1 complex (Figure S3). Consistent with anion recognition by operational chalcogen bonds, binding of nitrate ($TBANO_3$) was clearly weaker ($K_D = 6.2 \pm 0.4$ mM, selectivity $Cl^-/NO_3^- = 5.6$, Figure S4, Table S1). Binding of PF_6^- was not detectable (Figure S5).

Compared to **7**, chloride binding by **6** with only one cyano acceptor was clearly weaker ($K_D = 14.4 \pm 0.7$ mM). Anion binding by all DTTs with shallower σ holes was not detectable. Substitution of two cyano acceptors in **7** by sulfones in **10** did not much affect anion binding in THF ($K_D = 4.9 \pm 0.2$ mM, Cl^-/NO_3^-

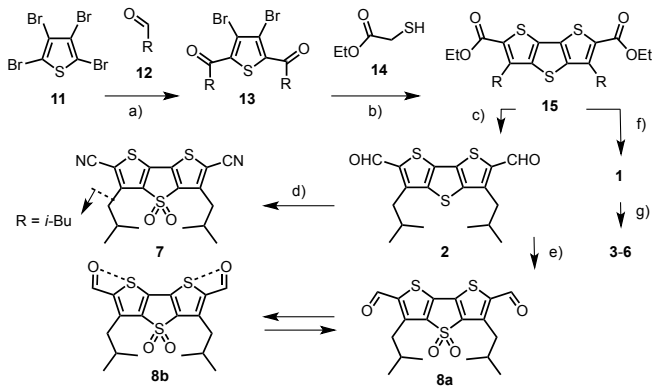

Scheme 1. (a) 1. BuLi, THF, –78 °C, 2 h, 69%; 2. $Na_2Cr_2O_7$, H_2SO_4, H_2O, acetone, rt, 16 h, 68%; (b) EtONa, EtOH, reflux, 2 h, 86%; (c) 1. DIBAL-H, THF, –78 °C, 30 min, quant; 2. Dess-Martin periodinane, CH_2Cl_2, rt, 2 h, 71%; (d) 1. NaN_3, TfOH, CH_3CN, 50 °C, 1 h, 71%; 2. mCPBA, $CHCl_3$, rt, 3 h, 77%; (e) mCPBA, $CHCl_3$, rt, 3 h, 36%; (f) 1. LiOH, EtOH, reflux, 16 h, 95%; 2. Ag_2CO_3, AcOH, DMSO, 120 °C, 16 h, 73%; (g) several steps, see SI.[17]

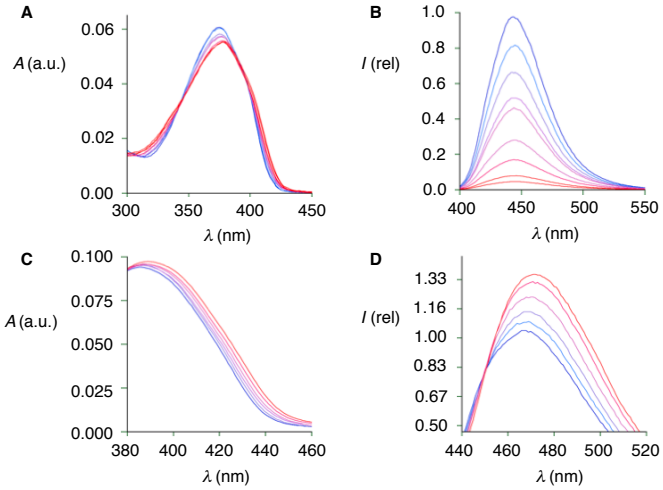

Figure 2. Absorption (A, C) and emission spectra (B, D, excitation at maxima) of **7** (A, B) and **8** (C, D) in THF in the presence of increasing concentrations of TBACl, from 0 mM (blue) to 20 mM (red).

= 2.6, Table S1). With two aldehyde acceptors DTT **8**, absorption (λ_{abs} = 389 nm) and emission (λ_{em} = 472 nm) increased with TBACl (Figures 2C, D). This hyperchromic response was consistent with competition from intramolecular chalcogen bonds in **8b** (Scheme 1). The theoretically predicted decrease in chloride affinity of **8** (Table 1, entry 8) was confirmed experimentally (K_D = 6.7 ± 0.7 mM).

Transport activities were assessed in large unilamellar vesicles (LUVs) composed of egg yolk phosphatidylcholine (EYPC) and loaded with 8-hydroxy-1,3,6-pyrenetrisulfonate (HPTS), a pH sensitive fluorescent probe.[18] With a base pulse, a pH gradient was applied first, then the transporters were added and their ability to accelerate the dissipation of the pH gradient was measured (Figures 3A, S6, S7). Activities were described by the effective concentration EC_{50} needed to reach 50% of the maximal activity Y_{max} (Figures S8, S9). For DTTs with methyl groups as substituents R^3, transport activities were poor. With one sulfone acceptor in **9**, EC_{50} = 27 ± 2 μM could be measured (Table 1, entry 9), DTT **10** with two sulfones was inactive (Table 1, entry 10). With evidence for comparably strong anion binding in THF secured (above), undetectable transport activity of DTT **10** was likely to originate from poor partitioning.

With isobutyl solubilizers as R^3, DTTs **1-4** with weak σ holes delivered nondescript EC_{50} around 20 μM (Table 1, entry 1-4). With the most powerful "sulfone" bridges in **5-7**, activities increased gradually with one and two additional cyano acceptor (Table 1, entries 5-7). The best EC_{50} = 1.9 ± 0.2 μM obtained for **7** coincided with the best K_D = 1.13 ± 0.03 mM for chloride binding in THF and the highest theoretical binding energy E_{int} = –34.6 kcal mol^{-1}, that is the deepest σ hole.

Hill coefficients were near n = 1 for all transporters (Table 1). Supported by curve fits and Job plots for anion binding in solution, this could suggest that DTTs transport anions as monomers.[19] Consistent with anion-selective transport, presumably anion/OH^- antiport,[18] the exchange of extravesicular anions affected transport activities overall more than the exchange of

Table 1. Anion Binding and Transport with Chalcogen Bonds.

cpds[a]	bridge	R^1	R^2	R^3	E_{int} (kcal mol^{-1})[b]	EC_{50} (μM)[c]	n[d]	Cl^-/NO_3^-[e]
1	S	H	H	*i*-Bu	–9.9	16 ± 3	1.3	–
2	S	CHO	CHO	*i*-Bu	–21.3 (–14.7)[f]	–[g]	–	–
3	SO	H	H	*i*-Bu	–16.6	19 ± 2	1.1	3.4
4	SO	CN	H	*i*-Bu	–24.0	22 ± 4	1.2	2.3
5	SO_2	H	H	*i*-Bu	–20.1	9.4 ± 0.6	1.5	2.2
6	SO_2	CN	H	*i*-Bu	–27.4	7 ± 2	1.4	2.0
7	SO_2	CN	CN	*i*-Bu	–34.6	1.9 ± 0.2	1.2	2.1
8	SO_2	CHO	CHO	*i*-Bu	–30.9 (–24.8)[f]	–[g]	–	–
9	SO_2	SO_2Et	H	Me	–26.8	27 ± 2	1.4	1.2
10	SO_2	SO_2Et	SO_2Et	Me	–32.7	–[g]	–	–

[a]Compounds, see Figure 1E for structures; bridge: Atoms bridging the two peripheral thiophenes in [3,2-b;2',3'-d]-DTTs. [b]Interaction energies for 1:1 chloride complexes computed at M062X/6-311G** level and BSSE corrected; R^3 = Me. [c]Effective concentration needed to reach 50% of maximal transport activity Y_{max} in the HPTS assay. [d]Hill coefficient of dose response curves in the HPTS assay. [e]Transport activity in the HPTS assay with extravesicular chloride compared to extravesicular nitrate. [f]Value in parenthesis for conformer **b** with competing intramolecular chalcogen bonds (Scheme 1). [g]Not detectable (fluorescence overlap, precipitation).

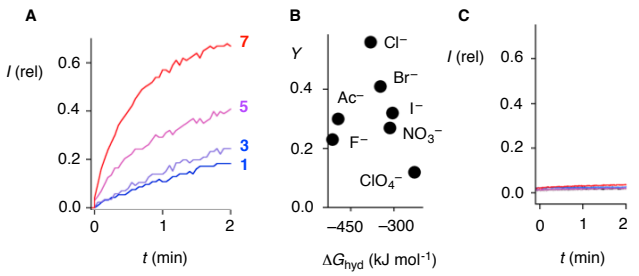

Figure 3. (A) Change in HPTS fluorescence (λ_{ex1} = 400 nm, λ_{ex2} = 450 nm) upon addition of **1**, **3**, **5** and **7** (10 μM) to EYPC LUVs with internal HPTS and a transmembrane pH gradient, calibrated to I = 1.0 after final lysis. (B) Dependence of transport activity Y of **7** on the nature of extravesicular anions (100 mM NaX, inside 100 mM NaCl). (C) Change in CF fluorescence (λ_{ex} = 492 nm) upon addition of **1**, **3**, **5** and **7** (10 μM) to EYPC LUVs with internal CF, calibrated to I = 1.0 after final lysis.

external cations (Figures 3B, S10). The obtained apparent anion selectivity sequences should not be overinterpreted because of the complexity of the assay (results for Ac^- and F^-, for example, are influenced by passive diffusion of their conjugate acids, Figure 3B). The consistently moderate activity with external nitrate was noteworthy because transporters that operate with anion-π interactions show high activity with external nitrate (Figures 3B, Table 1).[3,16,20] Relatively high LUMO energies down to E_{LUMO} = –3.70 eV obtained for DTT **7** from differential pulse voltammetry (DPV) firmly excluded any contributions for anion-π interactions to anion transport with chalcogen bonds (Figure S12; naphthalenediimide (NDI) anion-π transporters: E_{LUMO} < –4.00 eV, NDIs with –3.70 eV are π neutral[3,21]). The electrostatic potential confirmed that the π surface of the tricyclic moiety is not suitable for anion-π interactions, and that anion binding in the focal point of the σ holes on the proximal endocyclic sulfur atoms is clearly preferred (Figure 1H).

All new chalcogen-bond transporters were inactive in the CF assay (Figure 3C). These routine controls, operating on fluorescence recovery upon export of self-quenched 5(6)-carboxyfluorescein from CF-loaded EYPC LUVs,[18] excluded that more significant membrane damage from detergent effects and the like account for the activity observed in the HPTS assay.

In summary, the reported results provide compelling experimental and theoretical evidence for existence and significance of anion transporters that operate with chalcogen bonds and introduce DTTs as privileged motif to install chalcogen bonds in functional systems. Studies are ongoing to elaborate on these perspectives, particularly with regard to catalysis.[16]

■ ASSOCIATED CONTENT

Supporting Information. Detailed experimental procedures. This material is available free of charge via the Internet at http://pubs.acs.org.

■ AUTHOR INFORMATION

Corresponding Author
stefan.matile@unige.ch

Notes

The authors declare no competing financial interest.

■ ACKNOWLEDGMENTS

We thank the NMR and the Sciences Mass Spectrometry (SMS) platforms for services, A. Adibekian and D. Abegg for HRMS and the University of Geneva, the European Research Council (ERC Advanced Investigator), the Swiss National Centre of Competence in Research (NCCR) Chemical Biology, the NCCR Molecular Systems Engineering and the Swiss NSF for financial support.

■ REFERENCES

(1) (a) Fyles, T. M. *Acc. Chem. Res.* **2013**, *46*, 2847–2855. (b) Otis, F.; Auger, M.; Voyer, N. *Acc. Chem. Res.* **2013**, *46*, 2934–2943. (c) Valkenier, H.; Davis, A. P. *Acc. Chem. Res.* **2013**, *46*, 2898–2909. (d) Gokel, G. W.; Negin, S. *Acc. Chem. Res.* **2013**, *46*, 2824–2833. (e) Montenegro, J.; Ghadiri, M. R.; Granja, J. R. *Acc. Chem. Res.* **2013**, *46*, 2955–2965. (f) Barboiu, M.; Gilles, A. *Acc. Chem. Res.* **2013**, *46*, 2814–2823. (g) De Riccardis, F.; Izzo, I.; Montesarchio, D.; Tecilla, P. *Acc. Chem. Res.* **2013**, *46*, 2781–2790. (h) Davis, J. T.; Okunola, O.; Quesada, R. *Chem. Soc. Rev.* **2010**, *39*, 3843–3862. (i) Satake, A.; Yamamura, M.; Oda, M.; Kobuke Y. *J. Am. Chem. Soc.* **2008**, *130*, 6314–6315. (j) Jones, J. E.; Diemer, V.; Adam, C.; Raftery, J.; Ruscoe, R. E.; Sengel, J. T.; Wallace, M. I.; Bader, A.; Cockroft, S. L.; Clayden, J. Webb, S. J. *J. Am. Chem. Soc.* **2016**, *138*, 688–695. (k) Huo, Y.; Zeng, H. *Acc. Chem. Res.* **2016**, *49*, 922–930. (l) Wei, X.; Zhang, G.; Shen, Y.; Zhong, Y.; Liu, R.; Yang, N.; Al-mkhaizim, F. Y.; Kline, M. A.; He, L.; Li, M.; Lu, Z.-L.; Shao, Z.; Gong, B. *J. Am. Chem. Soc.* **2016**, *138*, 2749−2754. (m) Si, W.; Xin. P.; Li, Z.-T.; Hou, J.-L. *Acc. Chem. Res.* **2015**, *48*, 1612–1619. (n) Muraoka, T.; Endo, T.; Tabata, K, V.; Noji, H.; Nagatoishi, S.; Tsumoto, K.; Li, R.; Kinbara, K. *J. Am. Chem. Soc.* **2014**, *136*, 15584–15595. (o) Saha, T.; Dasari, S.; Tewari, D.; Prathap, A.; Sureshan, K. M.; Bera, A. K.; Mukherjee, A.; Talukdar, P. *J. Am. Chem. Soc.* **2014**, *136*, 14128–14135.

(2) Gale, P. A.; Busschaert, N.; Haynes, C. J. E.; Karagiannidis L. E.; Kirby, I. L. *Chem. Soc. Rev.* **2014**, *43*, 205–241.

(3) Vargas Jentzsch, A.; Hennig, A.; Mareda, J.; Matile, S. *Acc. Chem. Res.* **2013**, *46*, 2791–2800.

(4) (a) Beno, B. R.; Yeung, K.-S.; Bartberger, M. D.; Pennington, L. D.; Meanwell, N. A. *J. Med. Chem.* **2015**, *58*, 4383–4438. (b) Bauzà, A.; Mooibroek, T. J.; Frontera, A. *ChemPhysChem* **2015**, *16*, 2496–2517. (c) Ho, P. C.; Szydlowski, P.; Sinclair, J.; Elder, P. J. W.; Kubel, J.; Gendy, C.; Lee, L. M.; Jenkins, H.; Britten, J. F.; Morim, D. R.; Vargas-Baca, I. *Nat. Commun.* **2016**, *2*, 11299. (d) Kremer, A.; Fermi, A.; Biot, N.; Wouters, J.; Bonifazi, D. *Chem. Eur. J.* **2016**, *22*, 5665–5675. (e) Gsänger, M.; Kirchner, E.; Stolte, M.; Burschka, C.; Stepanenko, V.; Pflaum, J.; Würthner, F. *J. Am. Chem. Soc.* **2014**, *136*, 2351–2362.

(5) Getmanenko, Y. A.; Risko, C.; Tongwa, P.; Kim, E.-G.; Li, H.; Sandhu, B.; Timofeeva, T.; Bredas, J.-L.; Marder, S. R. *J. Org. Chem.* **2011**, *76*, 2660–2671.

(6) (a) Garrett, G. E.; Gibson, G. L.; Straus, R. N.; Seferos, D. S.; Taylor, M. S. *J. Am. Chem. Soc.* **2015**, *137*, 4126–4133. (b) Semenov, N. A. Lonchakov, A. V.; Pushkarevsky, N. A.; Suturina, E. A.; Korolev, V. V.; Lork, E.; Vasiliev, V. G.; Konchenko, S. N.; Beckmann, J.; Gritsan, N. P.; Zibarev, A. V. *Organometallics* **2014**, *33*, 4302–4314.

(7) Mishra, A.; Ma, C.-Q.; Bauerle, P. *Chem. Rev.* **2009**, *109*, 1141–1276.

(8) Kaes, C; Katz, A; Hosseini, M. W. *Chem. Rev.* **2000**, *100*, 3553–3590.

(9) Gaussian 09, Revision **D.01**, Frisch, M. J. *et al*. Gaussian, Inc., Wallingford CT, **2013**.[17]

(10) (a) Zhao, Y.; Truhlar, D. G. *J. Chem. Phys.* **2006**, *125*, 194101. (b) Zhao, Y.; Truhlar, D. G. *Theor. Chem. Acc.* **2008**, *120*, 215–241.

(11) (a) GaussView, Version 5, Dennington, R.; Keith, T.; Millam, J. *Semichem Inc.*, Shawnee Mission, KS, **2009**. (b) Electrostatic potential is projected on the 0.009 au electron density isosurface and its color-coding ranges between -0.012 au (red) and 0.07 au (blue).

(12) (a) Cinar M. E.; Ozturk, T. *Chem. Rev.* **2015**, *115*, 3036–3140. (b) Barbarella, G.; Di Maria, F. *Acc. Chem. Res.* **2015**, *48*, 2230–2241. (c) De Jong, F.; Janssen, M. J. *J. Org. Chem.* **1971**, *36*, 1645–1648. (d) He, X.; Borau-Garcia, J.; Woo, A. Y. Y.; Trudel, S.; Baumgartner, T. *J. Am. Chem. Soc.* **2013**, *135*, 1137−1147.

(13) (a) Frey, J.; Bond A. D.; Holmes, A. B. *Chem. Commun.* **2002**, *37*, 2424–2425. (b) Hong, W.; Yuan, H; Li, H.; Yang, X.; Gao, X.; Zhu, D. *Org. Lett.* **2011**, *13*, 1410–1413.

(14) Verolet, Q.; Rosspeintner, A.; Soleimanpour, S.; Sakai, N.; Vauthey, E.; Matile, S. *J. Am. Chem. Soc.* **2015**, *137*, 15644–15647.

(15) (a) Dado, G. P.; Gellman, S. H.; *J. Am. Chem. Soc.* **1993**, *115*, 12609–12610. (b) Sakai, N.; Gerard, D.; Matile, S. *J. Am. Chem. Soc.* **2001**, *123*, 2517–2524.

(16) (a) Cotelle, Y.; Benz, S.; Avestro, A.-J.; Ward, T. R.; Sakai, N.; Matile, S. *Angew. Chem. Int. Ed.* **2016**, *55*, 4275–4279. (b) Zhao, Y.; Cotelle, Y.; Avestro, A.-J.; Sakai, N.; Matile, S. *J. Am. Chem. Soc.* **2015**, *137*, 11582-11585.

(17) See SI.

(18) (a) Sakai, N.; Houdebert, D.; Matile, S. *Chem. Eur. J.* **2003**, *9*, 223–232. (b) Vargas Jentzsch, A.; Emery, D.; Mareda, J.; Nayak, S. K.; Metrangolo, P.; Resnati, G.; Sakai, N.; Matile, S. *Nat. Commun.* **2012**, *3*, 905.

(19) Bhosale, S.; Matile, S. *Chirality* **2006**, *18*, 849–856.

(20) (a) Adriaenssens, L.; Estarellas, C.; Vargas Jentzsch, A.; Martinez Belmonte, M.; Matile, S.; Ballester, P. *J. Am. Chem. Soc.* **2013**, *135*, 8324–8330. (b) Wang, D.-X.; Wang, M.-X. *J. Am. Chem. Soc.* **2013**, *135*, 892–897. (c) Giese, M.; Albrecht, M.; Ivanova, G.; Valkonen, A.; Rissanen, K. *Supramol. Chem.* **2012**, *24*, 48–55.

(21) (a) Miros, F. N.; Zhao, Y.; Sargsyan, G.; Pupier, M.; Besnard, C.; Beuchat, C.; Mareda, J.; Sakai, N.; Matile, S. *Chem. Eur. J.* **2016**, *22*, 2648–2657. (b) Miros, F. N.; Matile, S. *ChemistryOpen* **2016**, *5*, 219-226.

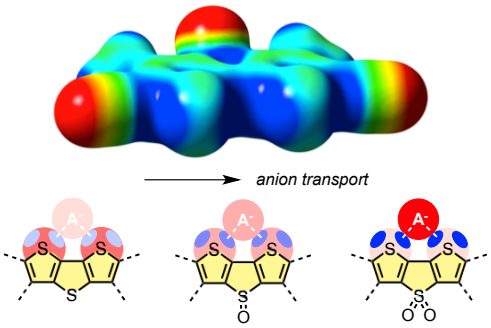
anion transport
A-
S
S
S
A-
S
S
S
O
A-
S
S
S
O O